

Follow Up Observations of Confirmed Exoplanets: WASP-49b, HAT-P-13, and WASP-140b

Shane Guernsey

*This work was submitted as part of a course requirement for completion of the BS degree in the Physics Program at RIT and, in its current form, does not appear in any publication external to RIT.**

(Dated: April 28, 2020)

Three exoplanets, WASP-49b, HAT-P-13b, and WASP-140b, were observed in order to follow up of system parameters reported by other literature. Science and calibration images were taken at Kitt Peak National Observatory using the WIYN 0.9m telescope from Jan. 5th to the 10th, 2020. Light curves were constructed from V and B band photometry, and from these light curves orbital periods of all planets were measured and planetary radii calculated from complete transits. WASP-49b was measured to have a period of (2.25 ± 0.26) days, HAT-P-13b had a period of (2.92 ± 0.29) days and a radius of $(1.35 \pm 0.27) R_J$. WASP-140b had an orbital period of (2.24 ± 0.01) days and a radius of $(1.26 \pm 0.09) R_J$. All measured features agreed with primary literature within one sigma error aside from the radius of WASP-140b, which agreed within 2 sigma error illustrating the utility of small telescopes for exoplanet followup.

Background

Exoplanet astronomy provides many exciting opportunities to observe objects that can inform theories of solar system formation and evolution. The most commonly detected type of exoplanets are gas giants called “Hot Jupiters” due to their size being up to several times the mass of Jupiter and their closeness to their host star. Other exoplanets can be water worlds similar to Neptune or terrestrial “Super Earths”, but due to their smaller sizes are much harder to detect from the ground via the commonly used transit technique.

The goal of this project was to measure transits of known exoplanet systems, and from those observations create light curves. From the constructed light curves features of the systems can be calculated such as radius of the planet, the orbital period, and the total transit duration. Once features of these systems are calculated, they will be compared to accepted values within the literature and discussed.

For ground-based observatories like the ones used in this project, exoplanets are best measured and studied using the transit photometry method. The only systems that can be detected via transit method are ones in which the planet crosses at least part way between the plane of the host star and our line of sight. As the planet crosses in front of the host, part of the light emitted from the star is blocked, which is observed as a decrease in brightness of the star. As the planet completes its transit, the star returns to its maximum brightness.

If the brightness of the star is measured for a sufficient length of time, one can compare the change in brightness during the transit of the host star which can be graphically represented with a light curve, as seen in Figure 1. Because the planet is much smaller than the host star, it does not take long for the planet to fully pass in front of the star which is shown by a steep drop in magnitude. And as it moves across the star it is still completely enveloped by the star’s silhouette shown by a flat bottom of the curve, then similar to the beginning of the curve

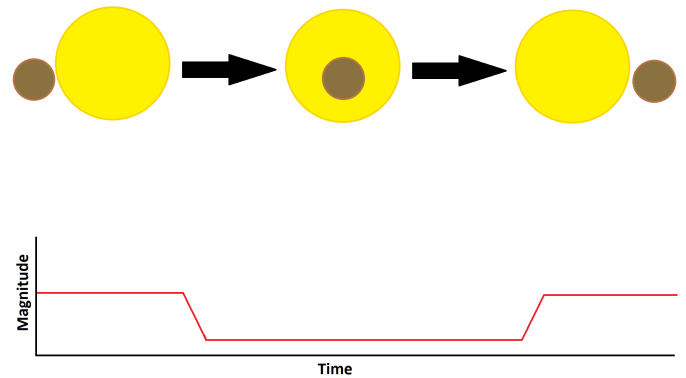


FIG. 1: An example light curve illustrating a gas giant passing in front of its host star.

the planet quickly leaves from the star’s path shown by a sharp increase in magnitude back to the star’s unobstructed brightness.

Exoplanet systems have not been frequently observed at the RIT Observatory due to having more requirements in order to observe these systems. Variation in magnitude caused by even the largest of exoplanets are still much smaller than other transient systems such as binaries, can combined with the unpredictable weather of Rochester, NY, the RIT Observatory has limitations on the systems it can view.

Kitt Peak National Observatory provides new opportunities to observe systems that cannot be seen at RIT, as access to the WIYN 0.9m provides a larger telescope that can detect fainter stars and smaller magnitude variations, its location on top of a mountain reduces atmospheric noise caused by higher airmass, and far more favorable weather conditions such as fewer clouds and lower humidity.

Last semester the first observation was conducted for this project on Sept. 19th, 2019, where the confirmed

exoplanet system of WASP-80 was observed. Unfortunately, the transit was not captured as the planet was not transiting that night. However, a previous exoplanet observation of TrEs-3b was provided by Dr. Michael Richmond, and from those observations a light curve was constructed.

The next step in the project for this semester was to calculate parameters of the systems from the constructed light curves. Additionally, the light curves for this semester would have been made from a combination of observations from Kitt Peak and RIT, but due to lab closures at RIT the observatory was no longer available.

The final step for this project is to compare the measured parameters to accepted values in primary literature and from the primary literature see what other parameters affect the outcomes of measurements on the systems.

Equipment

All observations for this work were done at Kitt Peak National Observatory in Tucson, Arizona over the week of January 5th to the 10th using the WIYN 0.9m telescope and a Half-Degree Imager (HDI) CCD camera, providing the possibilities of observing fainter targets than can be seen in Rochester NY. CCD stands for "Charge-Coupled Device", and the camera is an array of pixels on a silicon chip. A set of standardized Harris UBVRI filters were also used. Due to the size and architecture of the camera, a dedicated liquid nitrogen cooling system is built into the telescope in order to reduce the operating temperature of the CCD and thus reduce the dark current seen in the images. The HDI camera also has a shutter to control light exposure on the chip. This sets a minimum length on exposure length of images as the shutter needs time to open and close; it takes about half a second for the shutter to open and close.

Thermal noise and imperfections within the pixels are removed through the use of dark frames, which are taken by closing the camera shutter or covering the lens of the telescope and taking sets of images at an exposure length equal to that of the images that need to be dark subtracted. Another source of error is an offset that is added per pixel during CCD readout called bias. Bias calibration images are taken by blocking all light that could hit the CCD like in dark frames, but the bias frames are taken with a zero second exposure length. Because this bias is also found within the dark frames, taking bias frames can sometimes be skipped as the dark frames will also deal with this. Lastly, to account for a vignetting effect seen in images and dust throughout the optical system, flat field images are also taken by exposing the camera to a uniformly lit field and filling the pixel wells up to one-half to two-thirds of the full well depth. Over-exposure can cause counts to "spill" down the CCD and fill other pixels while causing the full pixels to clip and lose any significant information. This was avoided with carefully adjusted exposure times.



FIG. 2: A cleaned image from the second HAT-P-13 observation. The static-looking strip lining the bottom and right sides of the image are the overscan strips. In raw images, the strips blend in with the sky backgrounds and after cleaning the strips are cropped out of the final image. The FOV of the image is 29' by 29'.

Normally dark images are taken by closing the shutter to the camera and taking exposures at the same lengths as flat field images and the science images, but the HDI adds a section to every image called an overscan strip. The overscan strip is a thin section along a side and top or bottom of each image as seen in Figure 2. The overscan strip does not correlate to any real pixels in the CCD; these pixels are added in while the CCD is read out. Due to thermal noise and bias in the amplifier, these additional pixels will report counts as well, and those counts are used to subtract both dark current and bias counts from every image, removing the need to take sets of darks for every exposure length used for different sets of images.

Observations

From January 5th to January 10th four target systems were observed at Kitt Peak National Observatory in Tucson, Arizona. January 6th and 9th no observations were made, first for camera repairs on the 6th and then for poor weather on the 9th. The three successfully observed targets are listed in Table I, omitting K2-22 observed on the 8th.

Throughout the week there were minor but persistent shutter issues such as opening or closing at improper times that left small artifacts in the images, but most blemishes were either far enough away from the targets to not matter or images with significant issues were thrown

TABLE I: Spectral and ephemeris information on host stars and their exoplanets.

Target Info.	WASP-49	HAT-P-13	WASP-140
RA (hh:mm:ss)	06:04:21	08:39:32	04:01:33
Dec (dd:mm:ss)	-16:57:21	47:21:07	-20:27:04
V mag	11.36	10.6	12.1
B mag	N/A	11.34	11.83
Period (Days)	2.80	2.92	2.24
Transit Length (Hrs)	2.14 ± 0.01	3.23 ± 0.04	1.51 ± 0.02
Observation Date(s)	Jan. 5 th	Jan. 7 th , 10 th	Jan. 8 th
$R_{Star} (R_{\odot})$	0.9	1.56	0.87

out. On the 10th however there were significant shutter issues throughout the duration of the transit and a larger portion of images had to be discarded. On some night the telescope also suffered from some tracking issues as well, though these were dealt with by resetting the guide camera as needed.

In order to prepare for observational runs, targets must first be selected. The criteria each target must fit are the following:

- Targets must first be visible in the sky over Kitt Peak during the night.
- The Moon must not be in frame during the transit.
- Must be brighter than 18th magnitude.
- Must have a transit that can be observed in a single night
- Transit depth must be larger than the Signal-to-Noise ratio
- Preferably high in the sky during transit to reduce atmospheric error.

It is important to make sure the target is bright enough to not only be detected, but also have a deep enough transit to not be lost in the background noise. Because magnitude is measured on a logarithmic scale, a change in magnitude of say 0.1 is a lot larger if the host star has a magnitude of 10 versus a magnitude of 15.

One target, K2-22b has been identified as a Neptune-like planet, and is far smaller than the gas giants that were observed throughout the rest of the trip. Unfortunately, due to clouds, high wind, a very short transit length of about 30 minutes, and the very small expected magnitude change no transit could be extracted from the data collected. This did however inform future observations by setting a lower limit for transit depth and better planning for shorter transits of less than an hour.

While other targets had originally been planned for the first night of observations, due to viewing conditions WASP-49 was selected as the last portion of the transit was still in progress and out of the way of aforementioned issues. WASP-49 is a yellow-dwarf main sequence star with a confirmed exoplanet. Capturing only egress of the transit valuable measurements were still made. A list of comparison stars, or stars that do not vary in brightness

in the field of the target, used later on for photometry is shown in Table III. All comparison star tables are included in an appendix for ease of reference. For all transit targets, comparison star magnitudes are taken from the UCAC4 catalog through Aladin Sky Atlas¹. Figure 3 shows the finding chart for WASP-49 as well as the comparison stars used in the field. For the remainder of the transit, the night sky remained clear. Images were taken only in the V band as there was not enough time to plan for a second filter.

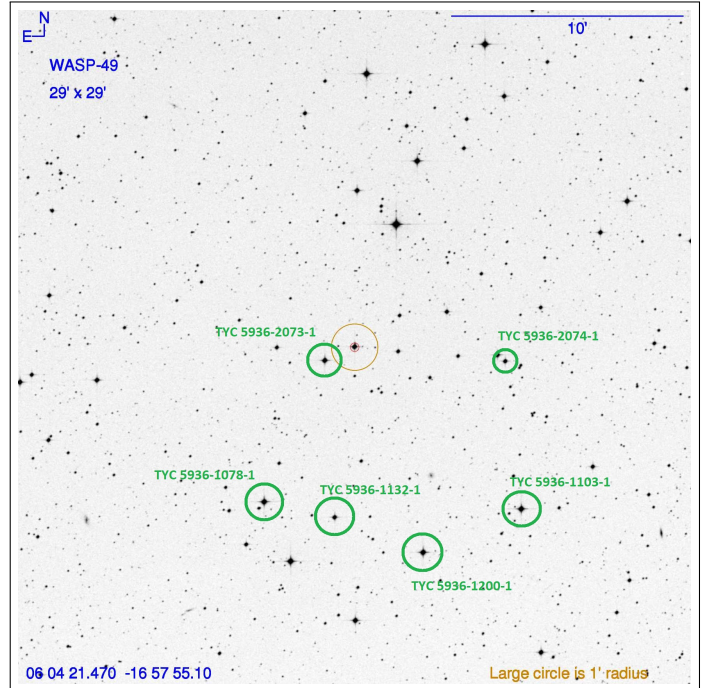


FIG. 3: Finding chart for WASP-49. Comparison stars are marked and labeled in green; WASP-49 is centered in the image in the yellow aperture. Right Ascension and Declination for WASP-49 are listed in the bottom left of the image. The FOV of the image is 29 by 29 arcmin.

HAT-P-13 is a G-type main sequence star that has two large confirmed exoplanets, however only HAT-P-13b is detectable through transit photometry. HAT-P-13 was selected as the observable exoplanet was making two transits during the trip, and this would allow for additional data on the same target and the opportunity to fold two light curves together, allowing for a higher resolution curve. Figure 4 shows the finding chart for HAT-P-13 along with the comparison stars used in photometry, whose information is listed in Table IV. The first night this target was observed the observation started a bit later than anticipated, but with a second night of data this issue was corrected. The first observation was done under clear skies, however on the second observation the moon was nearly within HAT-P-13's view. No issues were found in the resulting images from the second transit however aside from the aforementioned shutter issues. Both observations were done in both V and B band, alternating sets of images for the duration of the transit.

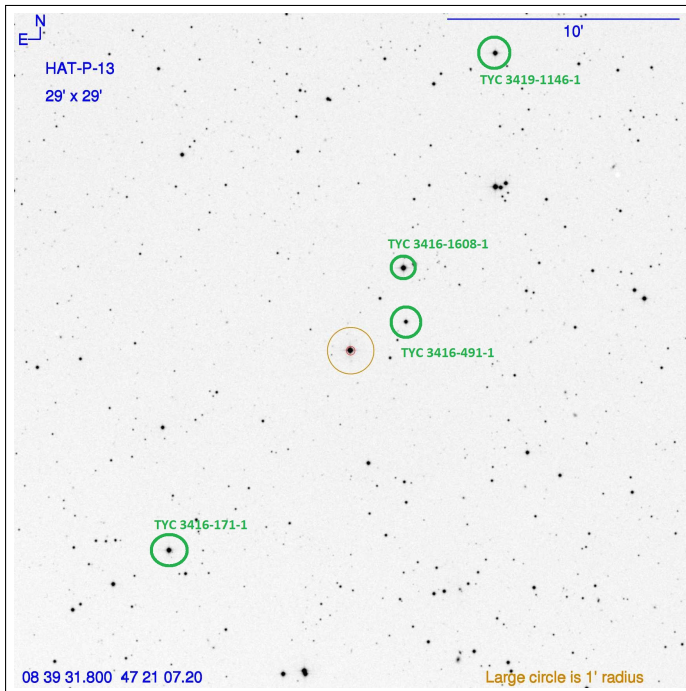


FIG. 4: Finding chart for HAT-P-13. Comparison stars are marked and labeled in green; HAT-P-13 is centered in the image in the yellow aperture. Right Ascension and Declination for HAT-P-13 are listed in the bottom left of the image. The FOV of the image is 29 by 29 arcmin.

The final target, WASP-140 is an orange-red main sequence star with a large exoplanet companion. This system was selected due to the expected transit depth being quite large. Figure 5 shows the finding chart for WASP-140 along with marked comparison stars later used in photometry. Table V contains information on the comparison stars for WASP-140. The sky remained clear for the duration of the transit and observations were done in both the B and V band filters.

Data Reduction

After all observations were complete, reduction of the science images began. Using AstroImageJ, all calibration and science images were checked for any unusual features or issues and images containing problems were omitted². Thanks to Dr. Andy Lipnicky, who produced a set of macros for AstroImageJ specifically for bias and dark subtracting the overscan strips from Kitt Peak images from the rest of their respective images, then cropping out the strip from the final product, the process was quick and painless.

To take an image, the CCD collects light for a set exposure time, filling the bins, then sends the accumulated charge towards the electronic amplifier and translated into a grid of pixels with counts of photons, which becomes our image. While one exposure is being read out, the CCD continues to collect counts for the next image.

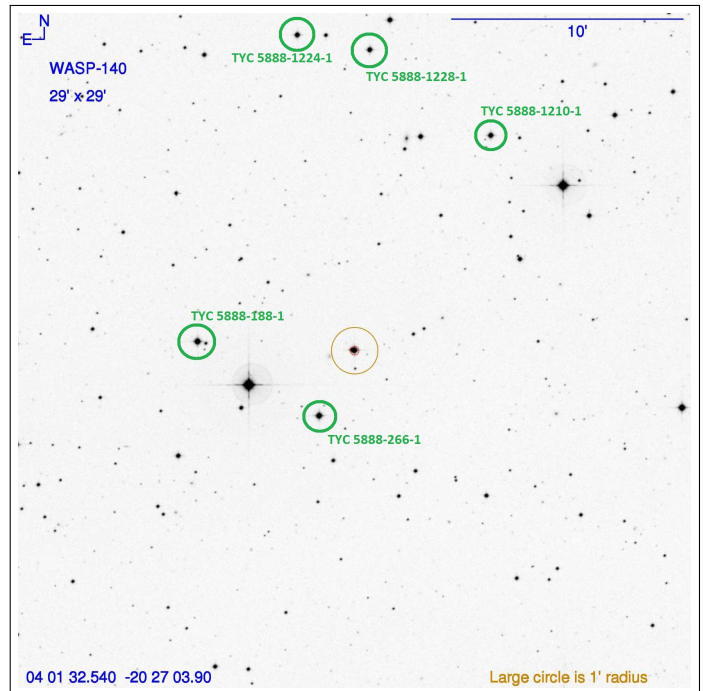


FIG. 5: Finding chart for WASP-140. Comparison stars are marked and labeled in green; WASP-140 is centered in the image in the yellow aperture. Right Ascension and Declination for WASP-140 are listed in the bottom left of the image. The FOV of the image is 29 by 29 arcmin.

After the flat field images were sorted by filter and dark current subtracted from them, the median of the sets of images were taken and a master flat was built. All science images were sorted by target and filter, then the overscan strips were used in each science image to remove the thermal noise and bias noise. The corresponding master flat was then divided out from each set of images.

Once all images were cleaned each set was aligned using AstroImageJ². To align the images, apertures must be selected that contain only the star they are placed on, and no other sources of light. The apertures must also include a good amount of sky background. Once aperture sizes were selected, a few apertures were placed on stars in the image including the target. Once the apertures were placed in one image, the program would automatically shift each subsequent image based on where the centroids of the selected stars move to. However, if the stars move too much between frames the program can lose track of the stars. So correct for this, alignment can be done in batches, then once each batch is aligned the batches can be aligned to one another. By aligning all images in a set photometry can be done much more easily than if the apertures had to be moved for each individual frame.

Analysis

To analyze the cleaned science images, multi-aperture photometry was performed. Photometry is the measure-

ment of light and how much is emitted over an area. Because only a change in brightness was being used, knowing the absolute flux emitted from a star is not necessary. This was measured by counting the number of photons collected from the target per unit area. This is only an apparent flux because much of the light from the target is lost along the path to our camera.

A. Multi-aperture Photometry

Multi-aperture photometry uses multiple apertures, or circles, placed on the target object and all other comparison objects in the image field. Then, all counts are integrated over the aperture area and from that flux can be calculated. The same aperture sizes were used that were selected during alignment, then placed on the target star and any comparison stars selected in the field. After the apertures were placed in the first image, the program ran through each image and output a measurement file containing Julian Dates, relative flux, source-sky backgrounds, magnitudes if inputted for some of the comparison stars, and errors for all calculated data. AstroImageJ uses Equation 1 to calculate relative flux:

$$relfluxT_j = \frac{F_T}{\sum_{i=1}^n F_{C_i}} \quad (1)$$

where F_T is the flux from the target star and F_{C_i} is the flux from each comparison star. The relative flux of each comparison star is also calculated by AstroImageJ using Equation 2:

$$relfluxC_j = \frac{F_{C_j}}{\sum_{i=1}^n F_{C_i}, i \neq j} \quad (2)$$

where j represents the aperture number of the comparison star and i indexes all aperture numbers.

Once AstroImageJ has the flux of all stars within the apertures, the magnitude of the selected objects can then be calculated using Equation 3:

$$m = C - 2.5 \log(F) \quad (3)$$

where C is the magnitude of the comparison star, and F is the flux of the object currently being measured. From the UCAC4 catalog the V and B band apparent magnitudes are extracted for the comparison stars in each image set and input into AstroImageJ². This process accounts for atmospheric effects such as airmass, wind, and clouds that can alter the amount of photons that reach the CCD and removes these variations. Once the process was complete, the output measurements file was then loaded into Python for further analysis.

B. Python

One issue that arises from using AstroImageJ is that the HJD values recorded in the .FITS files are rounded

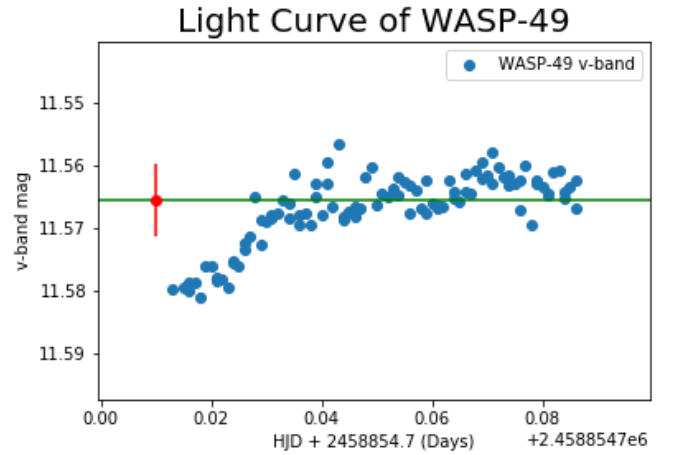


FIG. 6: Light curve for WASP-49b in the V filter. The blue line shows the average baseline magnitude for the host star. Brightness was measured in apparent magnitude. The red point is a characteristic error that represents the standard deviation of points around the green line.

to three decimal places after being run through the program. Because images are taken on timescales shorter than this, data points are plotted as though the image were taken at the same time. A workaround code was developed by RIT alumni Kaitlin Schmidt that can pull the HJD values directly from the FITS headers for entire sets of images.

This new set of times was then loaded into Python and light curves were constructed for the three targets. Ephemeris calculations are also accomplished in Python along with statistical analysis and error calculations.

Only the V-band light curves were used for ephemeris analysis as all three targets are brighter in the V band than the B band, and the B band light curves were used to check if the observed transits were caused by some other phenomena such as sunspots.

C. Light Curves

All measurable ephemerides are calculated from the constructed light curves. Important features of the light curve are the initial and final slopes and the midpoint of the transit. From ingress and egress the orbital period and transit length can be determined, and the midpoint of the transit give a total magnitude change that is used to calculate the radius of the planet.

Light curves constructed from multiple nights of observations can be folded together and plotted over the phase of the transit instead of the exact times. This allows for a clearer curve to be constructed and any variations in transit length, orbital period, or transit depth can be directly compared. This also can help to complete previous incomplete transits, such as the first observation of HAT-P-13b or WASP-49b. Phasing can also be done

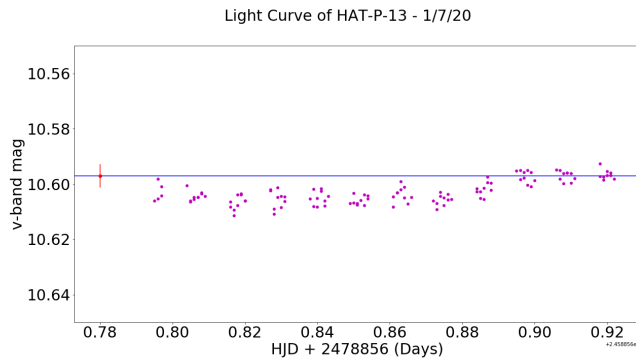


FIG. 7: Light curve for HAT-P-13b in the V filter on Jan. 7th. The blue line shows the average baseline magnitude for the host star. The red point is a characteristic error that represents the standard deviation of points around the green line.

with transits measured by other groups in order to compare times of transit points like ingress, mid transit, or egress.

1. WASP-49b

The end of WASP-49b's transit was captured, as seen in Figure 6. With the end of the transit, the orbital period of the planet was calculated by phasing the end of the light curve with the end of another observation, in this case the end of an observation done by Lendl et al³. From this, the phase of the light curve compared to the previous observation was calculated using Equation 4:

$$\phi = \frac{(HJD - HJD_o) \bmod P}{P} \quad (4)$$

where ϕ is the phase or what portion of the transit that has been completed, HJD is the transit date in question and HJD_o is the previous observation date, both in days, P is the period of the exoplanet, and modP is the modulus or fraction of the period that has been completed. From the equation above the period of WASP-49b was found to be (2.25 ± 0.26) days.

2. HAT-P-13b

HAT-P-13 was observed twice in two different filters; the light curves from Jan. 7th are shown in Figure 7 and Figure 8. Despite that the beginning of the transit was missed the full depth was observed and from this, and the second observation of HAT-P-13 caught the full transit as shown in Figures 9 and 10.

By finding the phase for each data point from the first observation compared to the second, both nights of data were folded together into one light curve that uses relative magnitude as a function of phase as shown in Figure

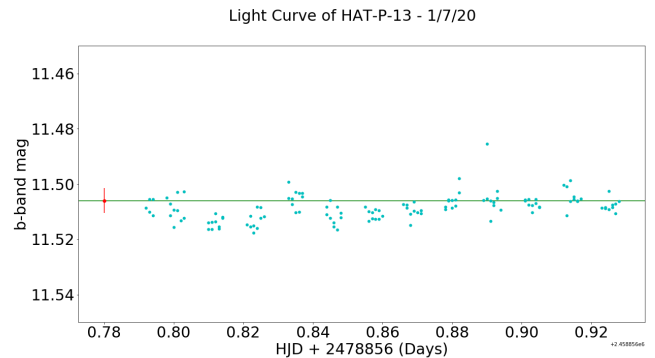


FIG. 8: Light curve for HAT-P-13b in the B filter on Jan. 7th. Format is the same as previous figures. Note the bump in the middle of the transit was observed in all stars in the images and is caused by atmospheric effects.

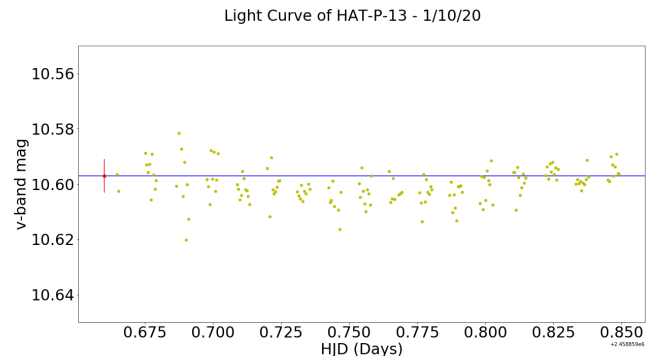


FIG. 9: Light curve for HAT-P-13b in the V filter on Jan. 10th. Format is the same as previous figures.

11. Because only a change in magnitude is needed to calculate planetary radius, the change in normalized magnitude can be used in the radius calculation. The period of HAT-P-13b was found to be (2.92 ± 0.29) days, and the radius of HAT-P-13b was found to be (1.35 ± 0.27) R_J , or Jupiter Radii.

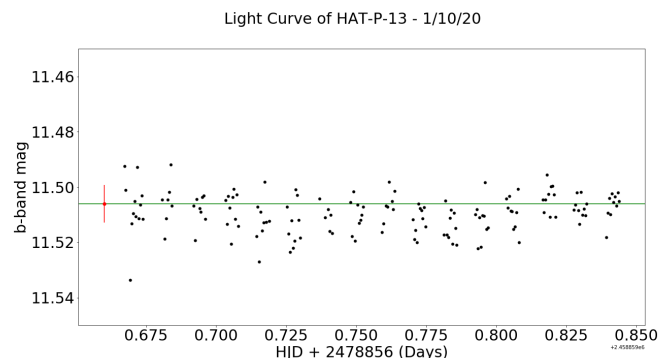


FIG. 10: Light curve for HAT-P-13b in the B filter on Jan. 10th. Format is the same as previous figures.

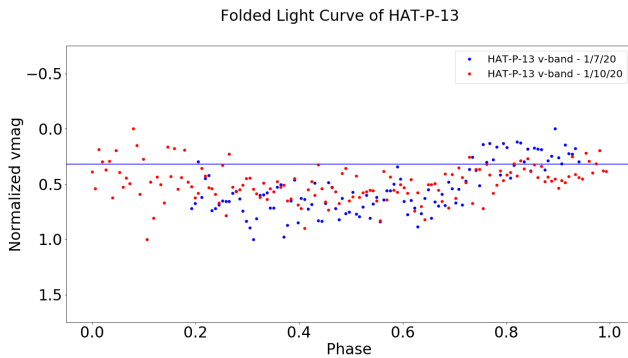


FIG. 11: Folded light curve of both observations of HAT-P-13. Magnitude was normalized and the transits were phased together. The blue line shows the host star’s magnitude without a transiting exoplanet.

3. WASP-140b

Lastly, WASP-140’s transit was fully captured in one run. Both V and B band light curves are shown in Figures 12 and 13. The period of WASP-140b was found to be (2.24 ± 0.01) days, and the radius of the planet was found to be $(1.26 \pm 0.09) R_J$.

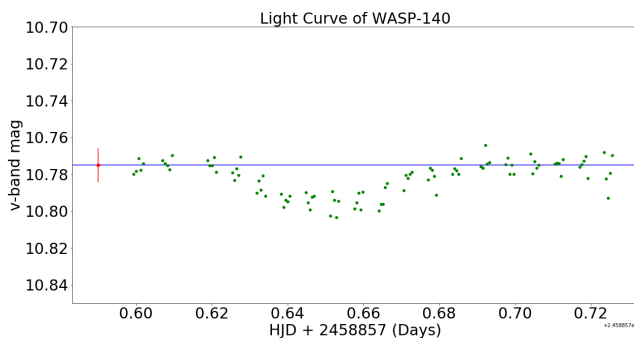


FIG. 12: Light curve for WASP-140b in the V filter. Format is the same as previous figures.

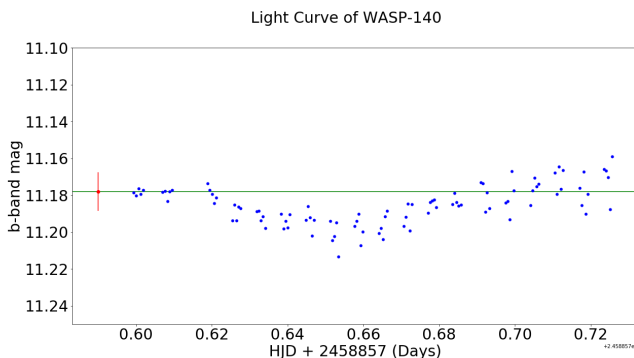


FIG. 13: Light curve for WASP-140b in the B filter. Format is the same as previous figures.

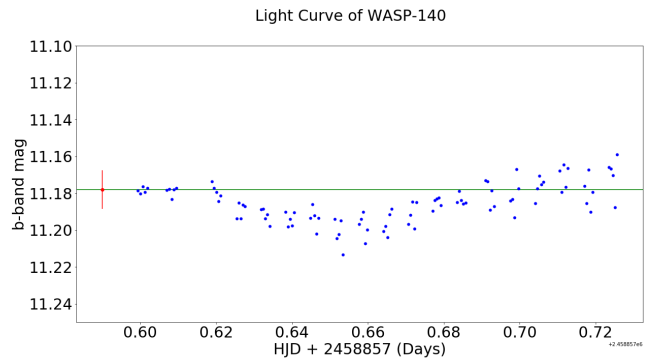


FIG. 14: Light curve for WASP-140b in the B filter. Format is the same as previous figures.

TABLE II: Calculated orbital period and planetary radius for all targets.

	WASP-49b	HAT-P-13b	WASP-140b
P (Days)	2.25 ± 0.26	2.92 ± 0.29	2.24 ± 0.01
Radius ($R_{Jupiter}$)	N/A	1.35 ± 0.27	1.26 ± 0.09

Discussion

Through transit photometry, a number of features can be extrapolated from the data such as the period and the radius of the orbiting body. The ration of the radii of the planet and the host star relate to the change in magnitude by Equation 5:

$$\Delta mag = \left(\frac{R_{Star}}{R_P} \right)^2 \quad (5)$$

where Δmag is the difference between the host star’s background magnitude and the magnitude at mid transit, R_{Star} is the radius of the host star, and R_P is the radius of the planet which can then be solved for using Equation 6:

$$R_P = R_{Star} \sqrt{\Delta mag} \quad (6)$$

All calculated parameters can be found in Table II.

All measurements made for the project were compared to primary literature referenced in the Kepler exoplanet database. Lendl et al. report a period for WASP-49b of $(2.7817387 \pm 5.6 \times 10^{-6})$ days which falls within one standard deviation of the measured value³. Lendl et al. also states that their radius for WASP-49b is $(1.115 \pm 0.047) R_J$ ³. In a future run the full transit of WASP-49b could be observed and the radius could be determined, as well as measuring the period of the planet with the previous observation made back in January.

For HAT-P-13b, Bakos et al. report a period of $(2.916206 \pm 1 \times 10^{-5})$ days and a radius of $(1.281 \pm 0.079) R_J$, both of which fall within one standard deviation of the measured values⁴. Bakos et al. mention

that the gravitational effect from the second planet in the system, HAT-P-13c, appears to have a not insignificant effect on HAT-P-13b as its periodicity is not constant⁴. Sada et al. state that HAT-P-13b also appears to only partially enter the optical path from the host star to Earth, in addition to long ingress and egress times of about 30 minutes⁵. This greatly increases the error of the mid transit point from ground-based observatories using transit photometry. This target is notoriously tricky to get very precise measurements on, so it is great that the measured features of the system were close to those reported by Bakos et al⁴.

Lastly, for WASP-140b Hellier et al. report a period of $(2.2359835 \pm 8 \times 10^{-7})$ days and a planetary radius of $1.44 (+0.42 / -0.18) R_J$ ⁶. While the period that was measured is within one standard deviation, the radius agreed within two. Hellier et al⁶. mention that WASP-140b is on a grazing transit with its host star, and that their measured radius may not be the true radius of the planet. They also mention that this planet appears to have only recently settled into its orbit based on its circularization time-scale being only about 100 Myr (Mega years), which is far shorter than the lifetime of its host star. That could lead to a future follow-up measurement, however different equipment and detection techniques would be required to perform the observation.

One of the biggest challenges of this project was trying to make sure as much error that could be removed as possible was, but error was introduced in just about every step of the process. With the observations one source of error was a build up of tracking and shutter issues with the telescope that were experienced in every observation.

Additionally, varying weather conditions caused for one strange pattern to appear in the first HAT-P-13 observation in the form of a bump in the middle of the transit. Luckily it was only prevalent in the B band observations which were not used in calculating the ephemerides of the exoplanet. A major source of post-observation error came from AstroImageJ as its comparison star flux calculations do not include the target star's flux which increases the relative flux of comparison stars.

Overall, considering all that has happened this semester this project was quite successful. From the results of this project more follow up measurements could be done on different parameters or to further refine the ones found here, as well as observe other confirmed exoplanet systems and parameterize those as well. Some important parameters would be impact parameter of the planet, which describes where the planet crosses the star relative to the star's center, full transit duration, and total distance the planet travels in front of its host star. These features can then help one determine orbital distance from the host star and give a clearer view of that solar system.

Acknowledgments

I would like to thank Dr. Jennifer Connelly, Dr. Michael Richmond, physics alumni Kain McCall, Kaitlin Schmidt, and Dr. Andy Lipnicky, Dr. Mishkatul Bhat-tacharya and the Capstone Committee for providing this opportunity and providing guidance and assistance throughout the project.

* Rochester Institute of Technology, School of Physics and Astronomy, Faculty Advisor: Dr. Jennifer Connelly

¹ F. Bonnarel *et al.*, *Astronomy and Astrophysics Supplement Series* **143**, 33 (2000).

² K. A. Collins, J. F. Kielkopf, K. G. Stassun, and F. V. Hessman, *The Astronomical Journal* **153**, 77 (2017).

³ M. Lendl *et al.*, *Astronomy & Astrophysics* **544**, A72 (2012).

⁴ G. Bakos *et al.*, *The Astrophysical Journal* **707**, 446 (2009).

⁵ P. V. Sada and F. G. Ramón-Fox, *Publications of the Astronomical Society of the Pacific* **128**, 024402 (2016).

⁶ C. Hellier *et al.*, *Monthly Notices of the Royal Astronomical Society* **465**, 3693 (2016).

⁷ W. Joye and E. Mandel, New features of saoiimage ds9, in *Astronomical data analysis software and systems XII* Vol. 295, p. 489, 2003.

I. APPENDIX

Comparison star properties for all exoplanet target analysis.

TABLE III: Comparison stars for WASP-49.

Star ID	RA	Dec	V mag	B mag
	<i>hh:mm:s</i>	<i>dd:mm:ss</i>		
TYC 5936-2073-1	06:03:6.8	-16:58m:30.3	11.35	11.93
TYC 5936-1078-1	06:04:37.8	-17:04:34.2	10.9	11.98
TYC 5936-1132-1	06:04:25.2	-17:05:14.9	11.96	12.15
TYC 5936-2074-1	06h:03:54.3	-16:58:33.3	12.27	13.12
TYC 5936-1103-1	06:03:51.5	-17:04:54.6	11.05	12.07
TYC 5936-1200-1	06:04:09.2	-17:04:54.6	11.05	12.07

TABLE IV: Comparison stars for HAT-P-13.

Star ID	RA	Dec	V mag	B mag
	<i>hh:mm:ss</i>	<i>dd:mm:ss</i>		
TYC 3416-491-1	08:39:17.8	47:22:23.8	11.94	12.75
TYC 3416-1608-1	08:39:18.7	47:24:42.2	10.74	11.22
TYC 3416-171-1	08:40:16.7	47:12:22.8	11.27	12.29
TYC 3419-1146-1	08:38:56.3	47:03:59.7	11.85	13.31

TABLE V: Comparison stars for WASP-140.

Star ID	RA	Dec	V mag	B mag
	<i>hh:mm:ss</i>	<i>dd:mm:ss</i>		
TYC 5888-266-1	04:01:39.2	-20:29:51.7	11.04	11.73
TYC 5888-188-1	04:02:01.4	-20:26:37.5	10.98	11.44
TYC 5888-1228-1	04:01:29.2	-20:14:10.8	11.49	11.92
TYC 5888-1210-1	04:01:07.1	-20:17:54.6	11.77	12.63
TYC 5888-1224-1	04:01:42.4	-20:13:30.6	11.46	13.4